

SCIENTIFIC REPORTS



OPEN

Selection of a novel DNA aptamer against OFA/iLRP for targeted delivery of doxorubicin to AML cells

Yacong An, Yan Hu, Xundou Li, Zhaoyi Li, Jinhong Duan & Xian-Da Yang

The standard treatment for most acute myeloid leukemia (AML) is chemotherapy, which is often associated with severe adverse effects. One strategy to reduce the adverse effects is targeted therapy that can selectively deliver anticancer drugs to tumor cells. Immature laminin receptor protein (OFA/iLRP) is a potential target for AML treatment, because it is over-expressed on the surface of AML cells but under-expressed in normal tissue. In this study, we developed the first aptamer for OFA/iLRP and explored its potential as a targeting ligand for delivery of doxorubicin (Dox) to AML cells *in vitro*. The selected aptamer (AB3) was a 59-base DNA oligonucleotides. It bound to OFA/iLRP structure with a K_d of 101 nM and had minimal cross-reactivity to albumin, trypsin, or ovalbumin. Moreover, AB3 could bind to OFA/iLRP-positive AML cells but not the OFA/iLRP-negative control cells. An aptamer-doxorubicin (Apt-Dox) complex was formed by intercalating doxorubicin into the DNA structure of AB3. Apt-Dox selectively delivered Dox to OFA/iLRP-positive AML cells but notably decreased the drug intake by OFA/iLRP-negative control cells. In addition, cytotoxicity study revealed that Apt-Dox efficaciously destroyed the OFA/iLRP-positive AML cells, but significantly reduced the damage to control cells. The results indicate that the OFA/iLRP aptamer AB3 may have application potential in targeted therapy against AML.

Acute myeloid leukemia (AML) is a serious threat to human health and accounts for about 147 thousands deaths globally in 2015¹. It is characterized by the rapid growth of immature myeloid precursors in bone marrow and blood². Despite the progress in biomedical sciences, AML still has a relatively poor clinical outcome. Among leukemic diseases that cause mortality in United States, AML is the most common type, with a 5-year survival of only 30–40%^{2,3}. The standard treatment for most AML at present is chemotherapy, which is often associated with severe side effects. Induction chemotherapy with cytarabine and anthracycline followed by consolidation chemotherapy has remained unchanged as the standard regimen for more than 3 decades⁴. In addition to killing leukemic cells, however, chemotherapeutics are also highly toxic to normal cells, causing serious adverse effects. Additionally, more than half of AML patients at diagnosis are older than 65 years, and frequently have antecedent hematologic disorders, adverse cytogenetic abnormalities, and other clinically significant comorbid conditions³. Consequently, aged patients often have poor tolerance to cytotoxic drugs with enhanced adverse effects⁵, and the median unadjusted overall survival of patients over 66 years is less than one year⁶. At present, there is an urgent need to develop novel AML therapeutic strategies that have decreased toxicity and improved efficacy.

Targeted therapy is a promising strategy for cancer treatment. By selective delivering chemotherapeutics to cancer cells rather than normal tissues, the undesirable side effects of conventional chemotherapy can be reduced, while the therapeutic efficacy is improved. It has been demonstrated that trastuzumab emtansine (T-DM1), an antibody-drug conjugate targeting human epidermal growth factor receptor 2 (HER2), prolonged progression-free survival (PFS) and overall survival (OS) compared with other anti-HER2 therapies in patients with HER2-positive metastatic breast cancer⁷. These studies indicate that targeted therapy has the potential to improve clinical outcome. For targeted AML treatment, gemtuzumab ozogamicin, a conjugation of anti-CD33 antibody and calicheamicin, was approved by FDA to treat patients with CD33-positive AML^{8,9}. Ideally, the molecular target employed in targeted therapy is tumor specific. It should be highly expressed in tumor but under-expressed in normal tissue, in order to generate a disparity in the amount of drug delivered to tumor vs. normal tissue. CD33, however, is expressed on both the normal myeloid cells and the leukemic cells. This drawback sometimes limited the application of gemtuzumab ozogamicin in clinical settings due to side effects¹⁰.

Institute of Basic Medical Sciences, Chinese Academy of Medical Sciences & Peking Union Medical College, Beijing, 100005, China. Correspondence and requests for materials should be addressed to X.-D.Y. (email: ayangmd@gmail.com)

For AML treatment, therefore, it is necessary to explore new targets that are highly expressed on AML cells but under-expressed in normal tissue.

Oncofetal antigen/immature laminin receptor protein (OFA/iLRP) is a potentially important molecular target for treatment of AML and other malignancies. OFA/iLRP is a 37 kD membrane protein that has been detected on the cell surface of various malignant tumors, but not on the surface of normal cells. OFA/iLRP is expressed in AML, colon cancer, fibrosarcoma, ovarian cancer, lung cancer, and cervical cancer^{11–15}. In normal tissues, OFA/iLRP is only expressed in embryonic and early fetal period, and disappears in later stages of development¹⁶. Barsoum *et al.* found that immunization with recombinant OFA/iLRP generated a significant antitumor effect in mice¹⁷, indicating that OFA/iLRP could be employed as a tumor-associated antigen in immunotherapy. Moreover, Scheiman *et al.* reported that treating tumor-bearing mice with short hairpin RNA (shRNA) against OFA/iLRP significantly inhibited tumor growth, suggesting that OFA/iLRP may be a potential target for gene therapy¹⁸. Importantly, OFA/iLRP expression is not only detected in many AML cell lines, but also in all clinical samples from AML patients¹¹. Furthermore, OFA/iLRP-specific cytotoxic T lymphocytes (CTLs) could lyse leukemic cells from patients with AML¹¹. These findings indicate that OFA/iLRP may potentially serve as an attractive molecular target for AML treatment. As mentioned above, OFA/iLRP has a molecular weight of about 37 kD, and is only expressed in embryonic or tumor cells. It should be noted that in mature tissues, two 37 kD OFA/iLRP molecules can form a dimer, generating a 67 kD protein named 67 LR or mature LRP¹⁹. The 67 LR is mainly localized in the cell membrane, and functions as a receptor for laminin²⁰. It also serves as receptors for viruses, bacteria, and prions at times^{21–23}. Numerous studies have shown that 67 LR is overexpressed in cancerous cells vs. their normal counterparts²⁴. The overexpression of 67 LR is associated with metastatic aggressiveness in many malignancies, including cancers of breast, lung, ovary, prostate, stomach and thyroid, as well as leukemia and lymphoma^{15,25–31}. Importantly, the expression of 67 LR in AML cells is significantly higher than that in normal myeloid cells³². Moreover, it has been reported that 67 LR expression shifted the characteristics of AML cells toward aggressive phenotype³³. Since both OFA/iLRP and its dimer 67 LR are overexpressed in AML cells, targeting OFA/iLRP appears a reasonable strategy for AML treatment.

Tumor-targeted therapy requires ligands that can bind specifically to tumor markers. In addition to antibodies, aptamers may also serve as tumor-targeting ligands. Aptamers are short oligonucleotides that can form complicated 3D structures with target-binding properties similar to antibodies³⁴. Moreover, aptamers have certain advantages as tumor-homing ligands, including low immunogenicity, better tumor penetration, easy chemical modification, and low production cost³⁵. Numerous studies have shown that aptamers can be used as ligands in chemical analyses and diagnostic applications^{36–38}. Aptamers can also be used as tumor-targeting ligands for delivery of doxorubicin or docetaxel to cancer cells^{39–41}. An aptamer drug (Macugen) has been approved by FDA for treatment of age-related macular degeneration. Other aptamer-based drugs, including E10030⁴², NOX-A12⁴³, and Pegpleranib⁴⁴, are being investigated in clinical trials. These facts indicate that aptamers have application potential in drug development.

To date, no aptamers against OFA/iLRP have been reported in literature. In this study, we developed the first DNA aptamer against OFA/iLRP and evaluated its binding affinity and specificity. Because doxorubicin is one of the most widely used chemotherapeutic agents, we also constructed an aptamer-doxorubicin complex (Apt-Dox) as an AML-targeted drug delivery system. We now report that Apt-Dox can selectively deliver doxorubicin to AML cells *in vitro*.

Results

Selection of aptamer against OFA/iLRP. In this study, a peptide from the extracellular domain of OFA/iLRP with the sequence of NQIQAAFREPR was chosen to be the target⁴⁵. This peptide represents an epitope that is exposed on the surface of the OFA/iLRP protein, according to studies of the crystal structure of the protein⁴⁶. Utilizing an epitope peptide as the target for aptamer selection has several advantages. First, synthetic peptides of high purity can be obtained in sufficient quantity, facilitating the process of aptamer selection. Second, the epitope is exposed on the surface of the protein, and thus may serve as a better target for aptamers. Prior studies have shown that aptamers with decent functionality can be developed using synthetic peptides as the selection target. Ferreira *et al.* selected an aptamer with a peptide representing the immunodominant region of MUC1. This aptamer has been shown capable of binding with multiple MUC1-expressing cancer cell lines⁴⁷. Liu *et al.* developed an aptamer using a peptide from the extracellular domain of HER2⁴⁰. This HER2 aptamer could recognize HER2-expressing breast cancer cells in clinical samples with similar efficiency and specificity as the FDA approved staining kit⁴⁸. Thus, it is feasible to employ a synthetic peptide as the target for aptamer selection.

The SELEX process is illustrated in Fig. 1A. The target peptide was conjugated covalently to the surface of magnetic beads. To select target-binding aptamers, the peptide-coated beads were incubated with a large variety of ssDNAs, and washed to remove the unbound DNA. The bead-bound DNA was eluted and amplified by PCR. The amplified dsDNA was separated into ssDNA which was used in the next round of selection. Flow cytometry was used to monitor the enrichment of OFA/iLRP aptamers. Compared with the initial ssDNA library, the binding to peptide-coated beads by selected DNA gradually strengthened with increasing rounds of selection (Fig. 1B). After eight rounds of selection, the enriched aptamer pool was cloned and analyzed. Among 120 clones, the aptamer AB3 showed relatively high capacity of binding to the OFA/iLRP-peptide. The sequence of this aptamer is 5'-TGCGTGTGTAGTGTGTCTGTTGTTTGTATTGTTGTCTATCCTCTTAGGGA TTTGGGCGG-3'.

Characteristics of the aptamer. Binding specificity is one of the most essential characteristics of an aptamer, and often evaluated by comparing the aptamer's bindings to the target molecule vs. several other control proteins. Albumin was often used as the control protein, because it is the most abundant protein in blood. Additionally, trypsin and OVA were also frequently employed as control proteins to test the binding specificity of the aptamers⁴⁰. To evaluate the binding specificity of the selected aptamer AB3, beads coated with OFA/

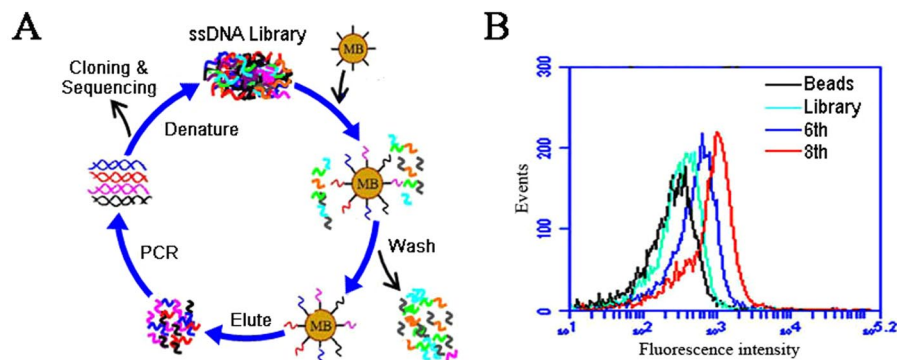


Figure 1. The process of aptamer selection. **(A)** Scheme of antigen based SELEX. The OFA/iLRP peptide-coated beads were incubated with ssDNA library, and washed to remove the unbound ssDNA. After heating at 95 °C for 5 min, the ssDNA still bound to the beads was eluted and amplified by PCR for next round of selection. In the last round of selection, the enriched target-binding ssDNA pool was cloned and sequenced to identify prospective OFA/iLRP aptamers. **(B)** Binding of the enriched ssDNA from the 6th and 8th round pools to beads coated with OFA/iLRP-peptide, as monitored by flow cytometry. The initial ssDNA library was used as the control.

iLRP-peptide, BSA, OVA, or trypsin were incubated with FAM-labeled aptamer, washed, and evaluated by flow cytometry. As presented in Fig. 2, aptamer AB3 showed a strong binding to the OFA/iLRP coated beads (Fig. 2A), whereas the bindings to BSA (Fig. 2B), OVA (Fig. 2C), or trypsin (Fig. 2D) coated beads were very weak. The results indicated that aptamer AB3 had a targeting specificity towards OFA/iLRP structure.

To quantitatively evaluate the binding affinity of AB3 to OFA/iLRP structure, the K_d value was estimated. Briefly, beads coated with OFA/iLRP-peptide were incubated with FAM-labeled AB3 of various concentrations, and evaluated for fluorescence intensity by flow cytometry. The K_d of the aptamer for binding with the OFA/iLRP-peptide was calculated to be 101.25 nM via non-linear regression analysis (Fig. 3).

Aptamer AB3 selectively bound to OFA/iLRP-expressing tumor cells. Although aptamer AB3 had certain binding affinity and specificity for OFA/iLRP-peptide, it was unknown whether the aptamer could also bind to OFA/iLRP-expressing cancer cells. To address this issue, OFA/iLRP-positive cells (HL-60, Jurkat, and Ramos) and OFA/iLRP-negative control cells (PBMC) were incubated separately with FAM-labeled aptamer, washed, and analyzed by flow cytometry. As presented in Fig. 4, the aptamer AB3 generated strong bindings to OFA/iLRP-positive cells (Fig. 4A–C), and bound weakly to OFA/iLRP-negative control cells (Fig. 4D). The results indicated that the AB3 aptamer could recognize and bind with the OFA/iLRP-positive cancer cells.

To further investigate the binding preference of aptamer AB3 to OFA/iLRP-positive and -negative cells, confocal microscopy were also used to study HL-60, Jurkat, Ramos, and PBMC cells treated by FAM-labeled aptamers. As shown in Fig. 4E, the fluorescence signal was observed mainly on the surface of OFA/iLRP-positive cells but not on OFA/iLRP-negative control cells. The results suggested that the aptamer AB3 could selectively bind with OFA/iLRP-positive cells, presumably by recognizing the extracellular domain of OFA/iLRP on these cells.

Aptamer AB3 targeted membrane proteins on the surface of OFA/iLRP-expressing cells. To further evaluate whether the aptamer targeted the extracellular domain of membrane proteins on OFA/iLRP-expressing cells, HL-60 cells were treated with trypsin or proteinase K for 5 min, incubated with FAM-labeled AB3, washed, and analyzed by flow cytometry. After trypsin or proteinase K treatment, the aptamer's binding to HL-60 cells was nearly abolished (Fig. 5). Based on the fact that the extracellular domains of membrane proteins, but not the other components of plasma membrane such as lipids and saccharides, were digested by trypsin or proteinase K⁴⁹, the flow cytometry results suggested that the aptamer probably targeted the extracellular domain of OFA/iLRP on the surface of cancer cells.

Formation of the aptamer-doxorubicin complex. Doxorubicin is one of the most extensively used drugs in chemotherapy and capable of inhibiting the proliferation of a wide variety of cancer cells. One of the acting mechanisms is that doxorubicin tends to intercalate into the DNA structures and interfere with the cellular functions⁵⁰. This mechanism can also be used to construct aptamer-doxorubicin complex, in that the drug can be readily inserted into the DNA structure of an aptamer to form a relatively stable complex. To study whether doxorubicin could intercalate into aptamer AB3, a fixed concentration of doxorubicin was mixed with increasing concentrations of AB3 at various ratios. Fluorescence spectroscopy was applied to monitor the mixtures, based on the fact that the red fluorescence of free doxorubicin will be quenched when the drug incorporates with DNA⁵¹. As shown in Fig. 6, with increasing aptamer/doxorubicin ratio, the fluorescence intensity of the mixture gradually decreased. When the Apt/Dox molar ratio increased to 0.25, the fluorescence largely reached the lowest level, indicating that, at this ratio, most doxorubicin had intercalated into the DNA structure of aptamer AB3, and that aptamer-doxorubicin complex (Apt-Dox) was formed.

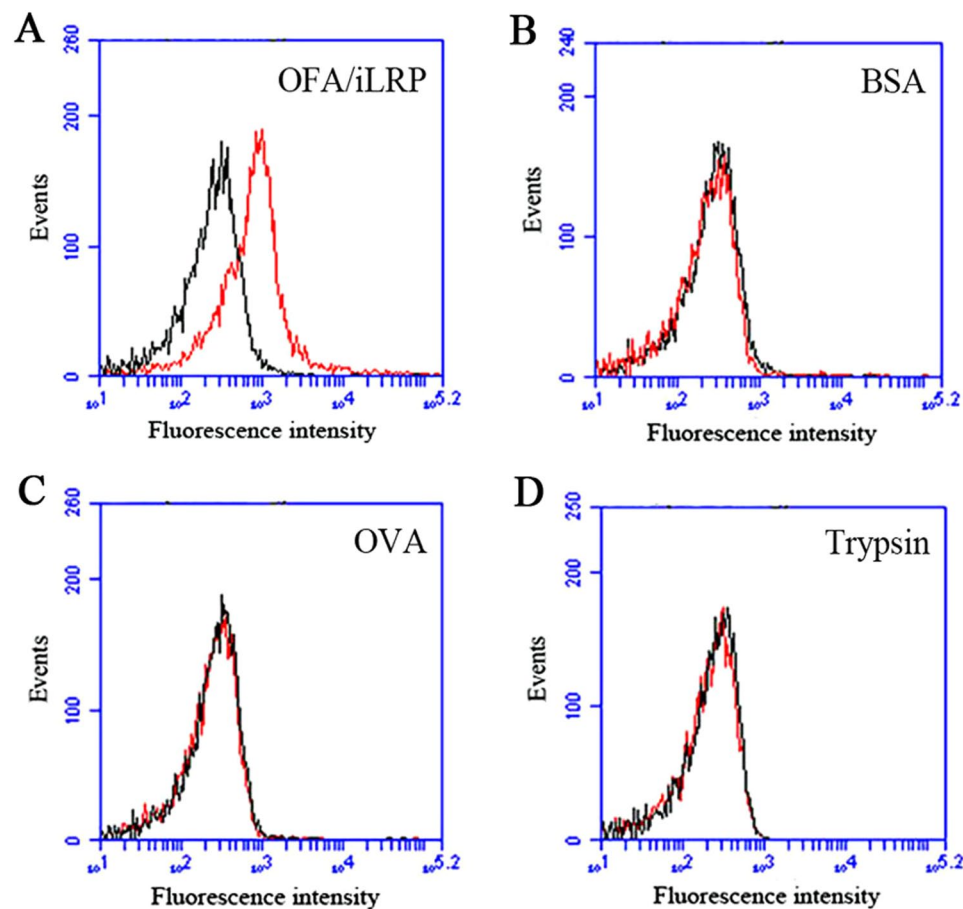


Figure 2. Binding properties of the AB3 aptamer. The bindings of FAM-labeled aptamer to OFA/iLRP-peptide (A), BSA (B), OVA (C), or trypsin (D) coated beads were analyzed by flow cytometry. The red curves represented the fluorescent signal of the aptamer AB3. The black curves represented the signal of initial ssDNA library, which served as the control here.

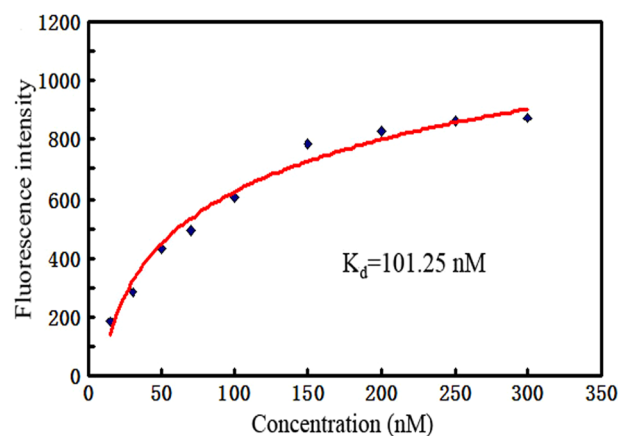


Figure 3. Evaluation of the aptamer's binding affinity to OFA/iLRP. FAM-labeled aptamer AB3 of various concentrations were incubated with OFA/iLRP peptide-coated beads, which were analyzed for fluorescence intensity by flow cytometry. The K_d was calculated based on values of fluorescence intensity obtained at various concentrations of aptamer.

Aptamer AB3 selectively delivered doxorubicin to OFA/iLRP-positive AML cells. With the formation of Apt-Dox complex, we next investigated whether the aptamer could selectively deliver Dox to OFA/iLRP-positive AML cells. Drug uptake studies were performed *in vitro*. Specifically, OFA/iLRP-positive AML cells

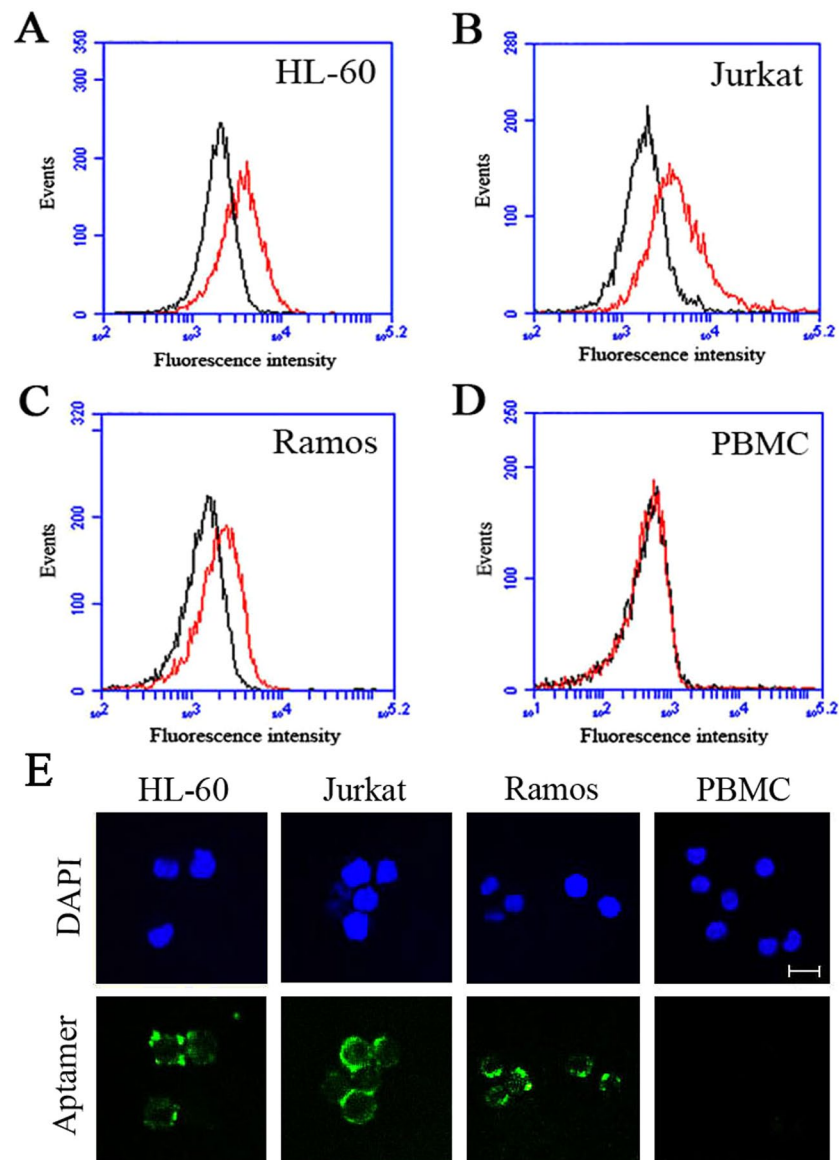


Figure 4. The bindings of aptamer AB3 to OFA/iLRP-positive and -negative cells. FAM-labeled AB3 were incubated with OFA/iLRP-positive cells HL-60 (A), Jurkat (B), or Ramos (C), and OFA/iLRP-negative cells PBMC (D). The cells were washed and analyzed by flow cytometry. The red curves represented the fluorescent signals of the aptamer and the black curves represented the control fluorescence signals generated by FAM-labeled initial ssDNA library. (E) Confocal microscopy evaluation of the aptamer's binding to OFA/iLRP-positive and -negative cells. Green fluorescence signals were generated by FAM-labeled aptamer. The nuclei were stained blue with DAPI. Bar represents 10 μ m.

(HL-60) and OFA/iLRP-negative control cells (PBMC) were incubated with free Dox or Apt-Dox separately and evaluated by confocal microscopy. As shown in Fig. 7, when treated with free Dox, both HL-60 and PBMC cells exhibited strong red fluorescence (Fig. 7, the upper panel), indicating that free Dox non-selectively entered both types of cells. When treated with Apt-Dox, however, the red fluorescence in HL-60 was much stronger than that in PBMC (Fig. 7, the bottom panel), indicating that Dox mostly entered HL-60 but not the control cells. Taken together, the data demonstrated that free Dox non-selectively diffused into most cells, while Apt-Dox selectively delivered Dox into OFA/iLRP-positive AML cells.

Apt-Dox generated a targeted cytotoxicity against the OFA/iLRP-positive AML cells. The above experiments indicated that Apt-Dox selectively delivered doxorubicin to OFA/iLRP-positive cells. We hypothesized that Apt-Dox would also generate a targeted cytotoxicity against the OFA/iLRP-positive leukemic cells. To test this postulate, HL-60 and PBMC cells were treated with free aptamer, free Dox, or Apt-Dox separately, and MTS assay was performed to analyze the cytotoxic effects of various treatments *in vitro*. As shown in Fig. 8, free Dox killed both the OFA/iLRP-positive and the OFA/iLRP-negative cells. By contrast, Apt-Dox largely destroyed

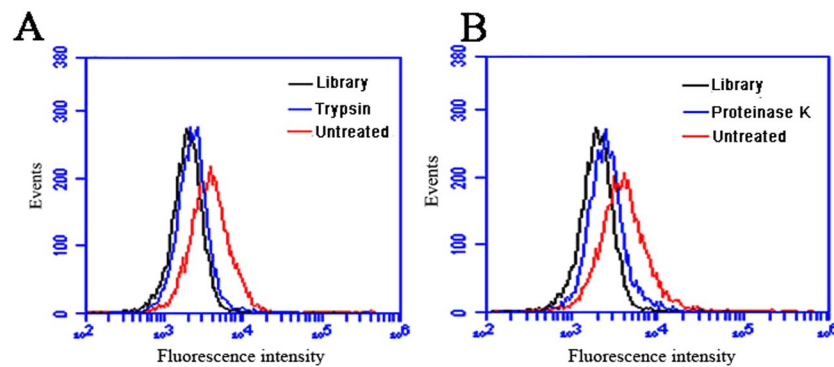


Figure 5. Effects of proteinase treatment on aptamer's binding to target cells. HL-60 cells were treated for 5 min with 0.25% trypsin (A) or 0.1 mg/mL proteinase K (B), washed with PBS, incubated with FAM-labeled aptamers, and analyzed with flow cytometry (blue lines). Digested cells treated with initial ssDNA library were used as the negative control (black lines). Untreated HL-60 cells incubated with FAM-labeled AB3 were used as the positive control (red lines).

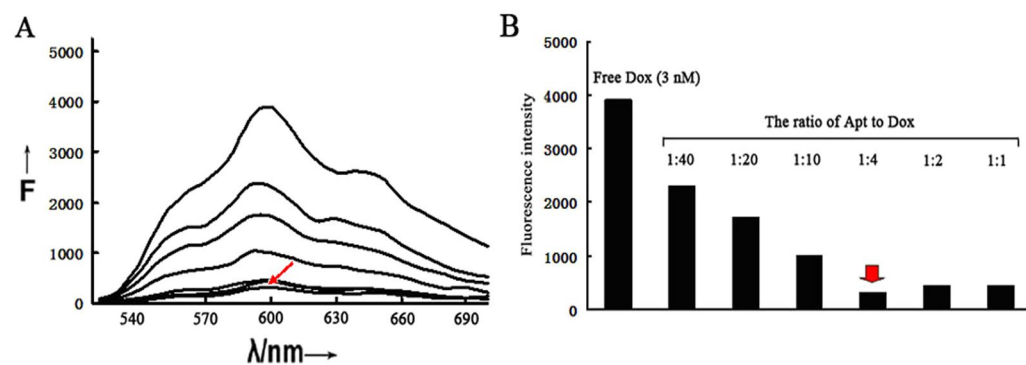


Figure 6. Fluorescence spectrum assessment of the aptamer-doxorubicin mixture. (A) Fluorescence spectra of doxorubicin solution mixed with increasing molar ratios of the aptamer (From top to bottom: 0, 0.025, 0.05, 0.1, 0.25, 0.5 and 1). (B) Fluorescence intensities of doxorubicin solution mixed with increasing molar ratios of the aptamer at $\lambda_{Em} = 600$ nm. The red arrow indicated the point whereby most doxorubicin molecules were loaded in the aptamers.

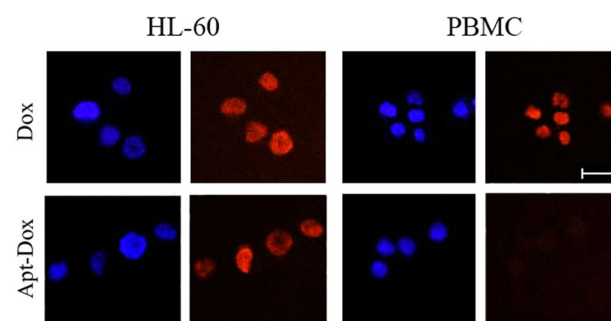


Figure 7. Cellular uptake of doxorubicin by OFA/iLRP-positive and -negative cells treated with free Dox or Apt-Dox. The OFA/iLRP-positive HL-60 cells and OFA/iLRP-negative PBMC were treated with free DOX (upper panel) or Apt-Dox (lower panel) separately for 2 h in PBS, and evaluated by confocal microscopy. The red fluorescence was generated by doxorubicin. The nuclei were stained blue with DAPI. Bar was 10 μ m.

the OFA/iLRP-positive HL-60 cells, but significantly reduced the damage to OFA/iLRP-negative control cells. Moreover, aptamer *per se* had no obvious cytotoxicity to either OFA/iLRP-positive or OFA/iLRP-negative cells, indicating that the aptamer was relatively nontoxic to both cell types. The results indicated that Apt-Dox generated a targeted cytotoxicity against the OFA/iLRP-positive AML cells, and simultaneously reduced the damage to OFA/iLRP-negative control cells.

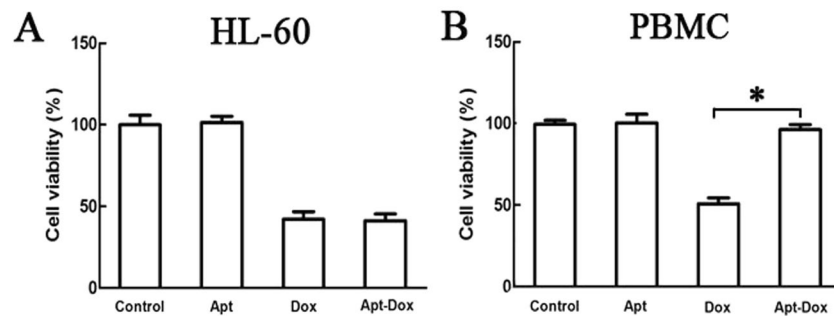


Figure 8. Cytotoxicity against OFA/iLRP-positive and -negative cells treated with Apt, Dox, or Apt-Dox. OFA/iLRP-positive cells HL-60 (A) and OFA/iLRP-negative cells PBMC (B) were incubated with aptamer, free Dox, or Apt-Dox for 4 hours, washed with PBS, and cultured for another 48 hours. MTS assay was employed to evaluate the cell viability (mean \pm SD, $n = 6$). The star indicated a statistically significant difference between the group treated with free Dox and that with Apt-Dox ($p < 0.01$).

Discussion

In this study, we selected the first aptamer for recognizing OFA/iLRP, which is a potential therapeutic target because it is over-expressed on the surface of AML cells but under-expressed in normal tissue. The aptamer AB3 could bind to OFA/iLRP-epitope with a K_d of 101.25 nM, and had minimal cross-reactivity to BSA, OVA, or trypsin (Figs 2, 3). Moreover, the aptamer bound strongly to OFA/iLRP-positive AML/lymphoma cells, but weakly to OFA/iLRP-negative control cells (Fig. 4). By intercalating doxorubicin into the DNA structure of AB3, an aptamer-doxorubicin complex (Apt-Dox) was constructed (Fig. 6). Confocal microscopy revealed that Apt-Dox could selectively deliver doxorubicin into AML cells (HL-60), while significantly reduced the drug intake by OFA/iLRP-negative control cells *in vitro* (Fig. 7). Moreover, cytotoxicity study showed that Apt-Dox generated robust killing of AML cells, but mitigated the damage to OFA/iLRP-negative control cells (Fig. 8). These results indicate that the OFA/iLRP aptamer may potentially serve as a tumor-homing ligand in targeted therapy against AML.

Targeting OFA/iLRP for drug delivery represents a new strategy for AML treatment. Currently, the main-stream treatment for most AML is still chemotherapy with cytotoxic agents. Although chemotherapeutics can suppress AML cells, damages to normal hematopoietic stem cells are common and associated with severe side effects. Targeted tumor therapy may potentially reduce the side effects, because cytotoxic agents are selectively delivered to tumor cells. For targeted AML treatment, an antibody-drug conjugate (gemtuzumab ozogamicin) has been developed, aiming at delivery of cytotoxic agents to CD33-expressing AML cells. However, since CD33 is also expressed on normal myeloid cells, gemtuzumab ozogamicin has been reported to cause severe side effects at times, limiting its clinical applications⁵². Therefore, new AML-targeting strategy is still warranted at present. OFA/iLRP is highly expressed on most AML cells but under-expressed in normal myeloid cells, and thus may potentially serve as a molecular target for selective drug delivery to AML. In this study, the OFA/iLRP aptamer selectively delivered doxorubicin to HL-60 AML cells, and reduced the drug intake by control cells *in vitro* (Figs 7, 8). Although this new strategy for AML treatment still needs further development, the results suggest that targeting OFA/iLRP for delivery of cytotoxic agents is theoretically feasible.

The mechanisms by which free doxorubicin or Apt-Dox enter the OFA/iLRP-positive AML cells and the control cells were probably different. Based on previous studies⁵³, we proposed the following hypothesis. For free doxorubicin, its lipophilic nature enabled the drug to diffuse into both types of cells with no selectivity. For Apt-Dox, doxorubicin was inserted within the DNA structure of aptamer and thus could not freely diffuse into cells. When OFA/iLRP-negative control cells were treated with Apt-Dox, the complex could not enter the cells, because both Apt-Dox and cell membrane were negatively charged and were repulsive to each other. When OFA/iLRP-positive AML cells were treated with Apt-Dox, however, the binding of the aptamer to OFA/iLRP on these cells could overcome the repulsive force and attach Apt-Dox to cell membrane. This led to the endocytosis of the Apt-Dox complex and the intake of doxorubicin by AML cells. Although this hypothesis may partially explain the targeting preference of Apt-Dox, further studies are warranted to reveal the detailed mechanism by which Apt-Dox selectively entered OFA/iLRP-positive AML cells.

It should be noted that, in addition to AML, OFA/iLRP is also widely expressed in other malignancies, and thus may potentially serve as a therapeutic target for a broader range of cancers. Holtl *et al.* reported that in an immunotherapy trial of renal cell carcinoma (RCC), OFA/iLRP-pulsed DC-based vaccine was well tolerated and had immunological as well as clinical effects in patients with metastatic RCC. The results indicated that OFA/iLRP might be an attractive candidate of tumor antigen for DC-based immunotherapy of RCC⁵⁴. Siegel *et al.* reported that a powerful immune reaction against B-cell leukemia could be induced in mice immunized with DCs transfected with the mRNA of OFA/iLRP, indicating that B-cell leukemia could be treated with immunotherapies based on OFA/iLRP¹¹. In this study, we also observed that the OFA/iLRP aptamer could bind to other types of tumor cells in addition to AML cells. Specifically, in addition to the AML cell line (HL-60), the aptamer was capable of recognizing T lymphocytic leukemia cells (Jurkat) and B-cell lymphoma cells (Ramos) as well (Fig. 4), consistent with prior studies demonstrating that Jurkat and Ramos cells were OFA/iLRP-positive¹¹. These findings suggest that, in addition to AML, targeting OFA/iLRP may also have potential for treatment of other malignancies.

In this study, an OFA/iLRP-binding aptamer was selected as the tumor-homing ligand. Although most targeted drug delivery systems employ antibodies as the tumor-homing ligand, aptamers also have great application potential in drug development as a new class of ligands. The US FDA has approved Macugen as the first aptamer drug for treatment of age-related macular degeneration⁵⁵. At present, there are several aptamer-based therapeutics that are under clinical trials of various phase^{56,57}. Aptamers have certain advantages of potential drug candidates or tumor-targeting ligands, including high affinity, excellent specificity, low immunogenicity, easy chemical modification, and low production cost. In order for aptamers to be utilized *in vivo*, they usually need to be chemically modified to resist digestion by nucleases. Therefore, future studies should focus on structural modifications of the OFA/iLRP aptamer, in order to improve its half-life for *in vivo* application. Future research should also address whether Apt-Dox still has the tumor-targeting anticancer effects *in vivo* with animal studies. Furthermore, the OFA/iLRP aptamer may also conjugate with drug-carrying nanoparticles to construct novel targeted drug delivery systems for AML treatment.

In conclusion, OFA/iLRP is widely expressed in AML and other types of malignancies, and may serve as a potential therapeutic target. In this study, we selected the first aptamer against OFA/iLRP, which may serve as a tumor-homing ligand for targeted therapy against OFA/iLRP-expressing tumors.

Methods

Cells and cultures. The OFA/iLRP-positive cell lines, HL-60 (human acute promyelocytic leukemia), Jurkat (human acute T lymphocyte leukemia), and Ramos (Burkitt's Lymphoma) were obtained from the Cell Center of Chinese Academy of Medical Sciences (Beijing, China). Peripheral Blood Mononuclear Cells (PBMC) were isolated from healthy donors. All cell lines were incubated in RPMI-1640 medium (Gibco) supplemented with 10% fetal bovine serum (FBS), 100 U/mL penicillin and 100 µg/mL streptomycin. Cells were grown in a humid atmosphere with 5% CO₂ at 37 °C. All donors were required to sign an informed consent. The protocol was approved by the Ethics Committee of Chinese Academy of Medical Sciences and Peking Union Medical College, and all methods were conducted in accordance with the Declaration of Helsinki.

Isolation of PBMC. Blood was collected from healthy donors in vacutainer containing sodium heparin. Five mL of blood was transferred into a 15 mL centrifuge tube (NEST) and diluted with equal volume of 0.9% sodium chloride. The diluted blood was aliquoted into two 15 mL centrifuge tubes containing 5 mL lymphocyte separation medium (Tbdscicece, China) and centrifuged at 1500 rpm/min for 20 min. Buffy coat containing PBMC was collected in 50 mL centrifuge tube and washed twice with 0.9% sodium chloride by centrifugation at 1500 rpm/min for 10 min. After discarding the supernatant, PBMC was resuspended with RPMI-1640 containing 10% FBS, 100 U/mL penicillin and 100 µg/mL streptomycin.

Reagents. Peptides of at least 95% purity were synthesized by Bootech (Shanghai, China). Bovine serum albumin (BSA) was purchased from Tbdscicece (Tianjin, China). Trypsin was purchased from Amresco (US). Ovalbumin (OVA) was purchased from Sigma (US). Oligonucleotide primers were synthesized by Invitrogen (Shanghai, China). Streptavidin-coated magnetic beads were purchased from Promega (US). Affimag UF magnetic microspheres (7–8 µm) were purchased from BaseLine ChromTech (Tianjin, China).

Immobilization of targets on magnetic beads. A peptide with the sequence of NQIQAAFREPR from the extracellular domain of OFA/iLRP was employed as the target for aptamer selection. The OFA/iLRP peptide was immobilized to epoxy magnetic beads by cross-linking of epoxy and amine groups. The epoxy magnetic beads (1×10^5) were washed thrice with 500 µL of Phosphate Buffered Saline (PBS), resuspended in 200 µL of Carbonate Buffer solution (CBS, PH = 10.7) containing OFA/iLRP peptide (2 µg), and incubated at room temperature with gentle stirring for 12 h. After washing thrice with 500 µL of PBS, the beads were stored at 4 °C in PBS. The conjugation of beads with other reagents (BSA, OVA, or trypsin) was accomplished similarly.

ssDNA library and primers. A 59-nt single strand DNA (ssDNA) library was used for aptamer selection. The ssDNA contained a central randomized sequence of 21-nt flanked by two 19-base sequences for primer annealing. The sequence was 5'-TGCGTGTGTAGTGTGTCTG(N21)CTCTTAGGGATTTGGGCGG-3'. A FAM-labeled forward primer, 5'-FAM-TGCGTGTGTAGTGTGTCTG-3' was used to monitor the binding of ssDNA with targets during selection process. When necessary, a biotin-labeled reverse primer, 5'-biotin-CCGCCAAATCCCTAA GAG-3', was used in PCR for later separation of the two chains of double-strand DNA (dsDNA) into ssDNA.

In vitro SELEX process. The initial ssDNA library (200 pmol) was dissolved in PBS, denatured at 95 °C for 5 min, and cooled immediately on ice for 15 min. The ssDNA was mixed with the OFA/iLRP peptide-coated magnetic beads in 200 µL PBS, which was shaken gently at room temperature for 50 min. The unbound ssDNA was discarded by washing the beads thrice with PBS. The target-bound ssDNA was eluted from beads by heating at 95 °C for 5 min and collecting the supernatant. The harvested oligonucleotides were amplified by PCR with FAM-labeled forward primer and biotin-labeled reverse primer (95 °C for 5 min, 18–24 cycles of 30 s at 95 °C, 30 s at 56 °C, and 40 s at 72 °C, and 72 °C for 10 min). The streptavidin-coated magnetic beads were mixed with PCR product, shaken for 20 min at room temperature, and washed with PBS. The dsDNA was denatured in alkaline condition (0.1 M NaOH) for 5 min. The beads were magnetically separated and discarded, to separate the bead-bound biotin-labeled antisense ssDNA from the FAM-labeled ssDNA in supernatant. The FAM-labeled ssDNA would be used for cytometric analysis or the next round selection. After eight rounds of selection, the enriched target-binding ssDNA pool was amplified by PCR with unmodified primers, and cloned into Escherichia coli using the TA cloning kit (Transgen) for DNA sequencing.

Flow cytometric analysis. OFA/iLRP peptide-, BSA-, OVA-, or trypsin-coated magnetic beads (2×10^5) were incubated with 20–40 pmol FAM-labeled ssDNA in 200 μ L PBS for 30 min at room temperature, washed once or twice with 200 μ L PBS, resuspended in 200 μ L PBS, and analyzed by flow cytometry (Accuri C6 Flow Cytometer, BD). Flow cytometry analysis of cells (2×10^5) was conducted in the similar way, except that the amount of ssDNA used was 40–60 pmol. To estimate the equilibrium dissociation constant (K_d) of the aptamer, magnetic beads coated with OFA/iLRP peptide were incubated with various concentrations of FAM-labeled aptamers and analyzed by flow cytometry. All experiments for binding assay were repeated for at least three times. The K_d was calculated by fitting the dependence of fluorescence intensity of specific binding on the concentration of the aptamers to the equation: $Y = B_{max} X / (K_d + X)$.

Confocal microscopic studies. HL-60, Jurkat, Ramos, or PBMC cells (2×10^5) were washed thrice with PBS and incubated with 60 pmol FAM-labeled aptamers in 300 μ L PBS for 30 min. After washing twice with PBS, the cells were fixed with 4% formaldehyde for 10 min at 4 °C. After washing cells twice again with PBS, cells were resuspended with 10 μ L of DAPI with the concentration of 1 μ g/ml for 5 min, mounted onto slide, and covered by a glass coverslip. The cells were imaged and analysed using a confocal fluorescence scanning microscopy (Perkin Elmer Ultraview, US).

Effects of proteinase treatment on aptamer binding to leukemic cells. HL-60 cells (2×10^5) were washed thrice with PBS and resuspended in 200 μ L of PBS containing 0.25% trypsin or 0.1 mg/mL proteinase K at 37 °C for 5 min. FBS was added to inhibit proteinase activity before washing cells twice with PBS. The cells were incubated with 60 pmol FAM-labeled aptamer in 300 μ L PBS for 30 min, washed with 200 μ L PBS, suspended with 200 μ L PBS, and analyzed by flow cytometry.

Drug-loading capacity of the aptamer. The aptamer was heated at 95 °C for 5 min and cooled immediately on ice for 15 min. Next, a fixed concentration of Dox (3 nM) was incubated with the aptamer at varying aptamer/Dox molar ratios (0, 0.025, 0.05, 0.1, 0.25, 0.5, and 1) respectively for 1 h in a 96-well black plate. Synergy4 analyzer was used to read the plate for assessing the fluorescence spectrum ($\lambda_{Ex} = 488$ nm, $\lambda_{Em} = 520$ –700 nm).

Cellular drug uptake studies. HL-60 or PBMC (3×10^5) were incubated with either 450 pmol doxorubicin or 112.5 pmol Apt-Dox complex in 300 μ L PBS for 2 h, washed twice with PBS, and fixed with 4% formaldehyde for 10 min at 4 °C. The cells were washed twice with PBS and mixed with 10 μ L of DAPI (1 μ g/ml) for 5 min. The cells were mounted onto slide, covered with a glass coverslip, and analyzed by confocal fluorescence scanning microscopy.

In vitro cytotoxicity studies. HL-60 or PBMC cells (5×10^4 cells per well) were grown in 96-well plates, treated with free doxorubicin at the final concentration of 0.2 μ M, Apt-Dox complex at the final concentration of 0.05 μ M, or aptamer at the final concentration of 0.05 μ M at 37 °C for 4 h, washed thrice with PBS, and cultured for an additional 48 h. Cell viability was determined by MTS assay according to the standard protocol as outlined by the manufacturer (Promega, US).

Statistical analysis. Statistical analysis was performed using the statistical SPSS 17.0 software. One-way ANOVA with Fisher's least significant difference (LSD) post hoc comparisons at 99% confidence interval was used for statistical comparisons. All data are presented as mean and standard deviation (mean \pm SD).

References

- Hay, S. I. *et al.* GBD 2015 Disease and Injury Incidence and Prevalence Collaborators. Global, regional, and national incidence, prevalence, and years lived with disability for 310 diseases and injuries, 1990–2015: a systematic analysis for the Global Burden of Disease Study 2015. *Lancet* **388**, 1545–1602, [https://doi.org/10.1016/S0140-6736\(16\)31678-6](https://doi.org/10.1016/S0140-6736(16)31678-6) (2017).
- Pulte, D., Gondos, A. & Brenner, H. Expected long-term survival of patients diagnosed with acute myeloblastic leukemia during 2006–2010. *Ann Oncol* **21**, 335–341, <https://doi.org/10.1093/annonc/mdp309> (2010).
- Miller, K. D. *et al.* Cancer treatment and survivorship statistics, 2016. *CA Cancer J Clin* **66**, 271–289, <https://doi.org/10.3322/caac.21349> (2016).
- Dohner, H., Weisdorf, D. J. & Bloomfield, C. D. Acute Myeloid Leukemia. *N Engl J Med* **373**, 1136–1152, <https://doi.org/10.1056/NEJMra1406184> (2015).
- Appelbaum, F. R. *et al.* Age and acute myeloid leukemia. *Blood* **107**, 3481–3485, <https://doi.org/10.1182/blood-2005-09-3724> (2006).
- Medeiros, B. C. *et al.* Big data analysis of treatment patterns and outcomes among elderly acute myeloid leukemia patients in the United States. *Ann Hematol* **94**, 1127–1138, <https://doi.org/10.1007/s00277-015-2351-x> (2015).
- Yan, H., Yu, K., Zhang, K., Liu, L. & Li, Y. Efficacy and safety of trastuzumab emtansine (T-DM1) in the treatment of HER2-positive metastatic breast cancer (MBC): a meta-analysis of randomized controlled trial. *Oncotarget* **8**, 102458–102467, <https://doi.org/10.18632/oncotarget.22270> (2017).
- Bross, P. F. *et al.* Approval summary: gemtuzumab ozogamicin in relapsed acute myeloid leukemia. *Clin Cancer Res* **7**, 1490–1496 (2001).
- Luger, S. M. How can one optimize induction therapy in AML? *Best Pract Res Clin Haematol* **30**, 301–305, <https://doi.org/10.1016/j.beha.2017.10.001> (2017).
- Godwin, C. D., Gale, R. P. & Walter, R. B. Gemtuzumab ozogamicin in acute myeloid leukemia. *Leukemia* **31**, 1855–1868, <https://doi.org/10.1038/leu.2017.187> (2017).
- Siegel, S. *et al.* Induction of cytotoxic T-cell responses against the oncofetal antigen-immature laminin receptor for the treatment of hematologic malignancies. *Blood* **102**, 4416–4423, <https://doi.org/10.1182/blood-2003-01-0198> (2003).
- Mafune, K. *et al.* Expression of a Mr 32,000 laminin-binding protein messenger RNA in human colon carcinoma correlates with disease progression. *Cancer Res* **50**, 3888–3891 (1990).
- Zuber, C. *et al.* Invasion of tumorigenic HT1080 cells is impeded by blocking or downregulating the 37-kDa/67-kDa laminin receptor. *J Mol Biol* **378**, 530–539, <https://doi.org/10.1016/j.jmb.2008.02.004> (2008).
- Poon, S. L., Klausen, C., Hammond, G. L. & Leung, P. C. 37-kDa laminin receptor precursor mediates GnRH-II-induced MMP-2 expression and invasiveness in ovarian cancer cells. *Mol Endocrinol* **25**, 327–338, <https://doi.org/10.1210/me.2010-0334> (2011).

15. Moodley, K. & Weiss, S. F. Downregulation of the non-integrin laminin receptor reduces cellular viability by inducing apoptosis in lung and cervical cancer cells. *PLoS One* **8**, e57409, <https://doi.org/10.1371/journal.pone.0057409> (2013).
16. Jackers, P. *et al.* Isolation from a multigene family of the active human gene of the metastasis-associated multifunctional protein 37LRP/p40 at chromosome 3p21.3. *Oncogene* **13**, 495–503 (1996).
17. Barsoum, A. L. *et al.* Production, safety and antitumor efficacy of recombinant Oncofetal Antigen/immature laminin receptor protein. *Biomaterials* **30**, 3091–3099, <https://doi.org/10.1016/j.biomaterials.2009.02.022> (2009).
18. Scheiman, J., Tseng, J. C., Zheng, Y. & Meruelo, D. Multiple Functions of the 37/67-kD Laminin Receptor Make It a Suitable Target for Novel Cancer Gene Therapy. *Molecular Therapy* **18**, 63–74, <https://doi.org/10.1038/mt.2009.199> (2010).
19. Landowski, T. H., Dratz, E. A. & Starkey, J. R. Studies of the structure of the metastasis-associated 67 kDa laminin binding protein: fatty acid acylation and evidence supporting dimerization of the 32 kDa gene product to form the mature protein. *Biochemistry* **34**, 11276–11287 (1995).
20. Malinoff, H. L. & Wicha, M. S. Isolation of a cell surface receptor protein for laminin from murine fibrosarcoma cells. *J Cell Biol* **96**, 1475–1479 (1983).
21. Akache, B. *et al.* The 37/67-kilodalton laminin receptor is a receptor for adeno-associated virus serotypes 8, 2, 3, and 9. *J Virol* **80**, 9831–9836, <https://doi.org/10.1128/jvi.00878-06> (2006).
22. Huang, S. H. & Jong, A. Evolving role of laminin receptors in microbial pathogenesis and therapeutics of CNS infection. *Future Microbiol* **4**, 959–962, <https://doi.org/10.2217/fmb.09.67> (2009).
23. Vana, K. *et al.* LRP/LR as an alternative promising target in therapy of prion diseases, Alzheimer's disease and cancer. *Infect Disord Drug Targets* **9**, 69–80 (2009).
24. Nelson, J. *et al.* The 67 kDa laminin receptor: structure, function and role in disease. *Biosci Rep* **28**, 33–48, <https://doi.org/10.1042/BSR20070004> (2008).
25. Menard, S., Tagliabue, E. & Colnaghi, M. I. The 67 kDa laminin receptor as a prognostic factor in human cancer. *Breast Cancer Res Tr* **52**, 137–145 (1998).
26. Song, T. *et al.* Expression of 67-kDa laminin receptor was associated with tumor progression and poor prognosis in epithelial ovarian cancer. *Gynecol Oncol* **125**, 427–432, <https://doi.org/10.1016/j.ygyno.2012.01.030> (2012).
27. Waltregny, D. *et al.* Detection of the 67-kD laminin receptor in prostate cancer biopsies as a predictor of recurrence after radical prostatectomy. *Eur Urol* **40**, 495–503 (2001).
28. Liu, L. L. *et al.* Hypoxia promotes metastasis in human gastric cancer by up-regulating the 67-kDa laminin receptor. *Cancer Science* **101**, 1653–1660, <https://doi.org/10.1111/j.1349-7006.2010.01592.x> (2010).
29. Montuori, N. *et al.* Laminin receptors in differentiated thyroid tumors: restricted expression of the 67-kilodalton laminin receptor in follicular carcinoma cells. *J Clin Endocrinol Metab* **84**, 2086–2092, <https://doi.org/10.1210/jcem.84.6.5721> (1999).
30. Montuori, N. *et al.* Expression of the 67-kDa laminin receptor in acute myeloid leukemia cells mediates adhesion to laminin and is frequently associated with monocytic differentiation. *Clin Cancer Res* **5**, 1465–1472 (1999).
31. Carbone, A., Gloghini, A., Colombatti, A., Castronovo, V. & Menard, S. Expression of the Monomeric 67-Kd Laminin-Binding Protein in Human Lymphomas as Defined by Mluc5 Monoclonal-Antibody and Paraffin Section Immunohistochemistry. *Hum Pathol* **26**, 541–546 (1995).
32. Montuori, N. *et al.* 67 kDa laminin receptor (67 LR) in normal and neoplastic hematopoietic cells: is its targeting a feasible approach? *Transl Med UniSa* **15**, 8–14 (2016).
33. Ando, K. *et al.* High expression of 67-kDa laminin receptor relates to the proliferation of leukemia cells and increases expression of GM-CSF receptor. *Exp Hematol* **39**, 179–186 e174, <https://doi.org/10.1016/j.exphem.2010.11.001> (2011).
34. Tuerk, C. & Gold, L. Systematic evolution of ligands by exponential enrichment: RNA ligands to bacteriophage T4 DNA polymerase. *Science* **249**, 505–510 (1990).
35. Liu, J. *et al.* Recent developments in protein and cell-targeted aptamer selection and applications. *Curr Med Chem* **18**, 4117–4125, BSP/CMC/E-Pub/2011/ 309 (2011).
36. Pu, Y. *et al.* Using DNA aptamer probe for immunostaining of cancer frozen tissues. *Anal Chem* **87**, 1919–1924, <https://doi.org/10.1021/ac504175h> (2015).
37. Zamay, G. S. *et al.* Aptamers Selected to Postoperative Lung Adenocarcinoma Detect Circulating Tumor Cells in Human Blood. *Mol Ther* **23**, 1486–1496, <https://doi.org/10.1038/mt.2015.108> (2015).
38. Hu, Y. *et al.* Novel MUC1 aptamer selectively delivers cytotoxic agent to cancer cells *in vitro*. *PLoS One* **7**, e31970, <https://doi.org/10.1371/journal.pone.0031970> (2012).
39. Farokhzad, O. C. *et al.* Targeted nanoparticle-aptamer bioconjugates for cancer chemotherapy *in vivo*. *Proc Natl Acad Sci USA* **103**, 6315–6320, <https://doi.org/10.1073/pnas.0601755103> (2006).
40. Liu, Z. *et al.* Novel HER2 aptamer selectively delivers cytotoxic drug to HER2-positive breast cancer cells *in vitro*. *J Transl Med* **10**, 148, <https://doi.org/10.1186/1479-5876-10-148> (2012).
41. Yu, C. *et al.* Novel aptamer-nanoparticle bioconjugates enhances delivery of anticancer drug to MUC1-positive cancer cells *in vitro*. *PLoS One* **6**, e24077, <https://doi.org/10.1371/journal.pone.0024077> (2011).
42. Jaffe, G. J. *et al.* Dual Antagonism of PDGF and VEGF in Neovascular Age-Related Macular Degeneration: A Phase IIb, Multicenter, Randomized Controlled Trial. *Ophthalmology* **124**, 224–234, <https://doi.org/10.1016/j.ophtha.2016.10.010> (2017).
43. Poolsup, S. & Kim, C. Y. Therapeutic applications of synthetic nucleic acid aptamers. *Curr Opin Biotechnol* **48**, 180–186, <https://doi.org/10.1016/j.copbio.2017.05.004> (2017).
44. Drolet, D. W., Green, L. S., Gold, L. & Janjic, N. Fit for the Eye: Aptamers in Ocular Disorders. *Nucleic Acid Ther* **26**, 127–146, <https://doi.org/10.1089/nat.2015.0573> (2016).
45. Jamieson, K. V., Wu, J., Hubbard, S. R. & Meruelo, D. Crystal structure of the human laminin receptor precursor. *J Biol Chem* **283**, 3002–3005, <https://doi.org/10.1074/jbc.C700206200> (2008).
46. Jamieson, K. V., Hubbard, S. R. & Meruelo, D. Structure-Guided Identification of a Laminin Binding Site on the Laminin Receptor Precursor. *Journal of Molecular Biology* **405**, 24–32, <https://doi.org/10.1016/j.jmb.2010.10.028> (2011).
47. Ferreira, C. S., Matthews, C. S. & Missailidis, S. DNA aptamers that bind to MUC1 tumour marker: design and characterization of MUC1-binding single-stranded DNA aptamers. *Tumour Biol* **27**, 289–301, <https://doi.org/10.1159/000096085> (2006).
48. Chu, M. *et al.* Evaluation of human epidermal growth factor receptor 2 in breast cancer with a novel specific aptamer. *Cell Mol Immunol* **14**, 398–400, <https://doi.org/10.1038/cmi.2015.31> (2017).
49. Rong, Y. *et al.* Identification of an aptamer through whole cell-SELEX for targeting high metastatic liver cancers. *Oncotarget* **7**, 8282–8294, <https://doi.org/10.18632/oncotarget.6988> (2016).
50. Bagalkot, V., Farokhzad, O. C., Langer, R. & Jon, S. An aptamer-doxorubicin physical conjugate as a novel targeted drug-delivery platform. *Angew Chem Int Edit* **45**, 8149–8152, <https://doi.org/10.1002/anie.200602251> (2006).
51. Goodman, R. P. *et al.* Rapid chiral assembly of rigid DNA building blocks for molecular nanofabrication. *Science* **310**, 1661–1665, <https://doi.org/10.1126/science.1120367> (2005).
52. Petersdorf, S. H. *et al.* A phase 3 study of gemtuzumab ozogamicin during induction and postconsolidation therapy in younger patients with acute myeloid leukemia. *Blood* **121**, 4854–4860, <https://doi.org/10.1182/blood-2013-01-466706> (2013).
53. Hu, Y., Li, X., An, Y., Duan, J. & Yang, X. D. Selection of a novel CD19 aptamer for targeted delivery of doxorubicin to lymphoma cells. *Oncotarget* **9**, 26605–26615, <https://doi.org/10.18632/oncotarget.24902> (2018).

54. Holtl, L. *et al.* Immunotherapy of metastatic renal cell carcinoma with tumor lysate-pulsed autologous dendritic cells. *Clin Cancer Res* **8**, 3369–3376 (2002).
55. Ng, E. W. *et al.* Pegaptanib, a targeted anti-VEGF aptamer for ocular vascular disease. *Nat Rev Drug Discov* **5**, 123–132, <https://doi.org/10.1038/nrd1955> (2006).
56. Zhou, J. H. & Rossi, J. Aptamers as targeted therapeutics: current potential and challenges. *Nature Reviews Drug Discovery* **16**, 440–440, <https://doi.org/10.1038/nrd.2017.86> (2017).
57. Nimjee, S. M., White, R. R., Becker, R. C. & Sullenger, B. A. Aptamers as Therapeutics. *Annu Rev Pharmacol* **57**, 61–79, <https://doi.org/10.1146/annurev-pharmtox-010716-104558> (2017).

Acknowledgements

This work was supported by the Ministry of Science and Technology (2017YFA0205501), the Natural Science Foundation of China (81572997, 81602712), the CAMS Innovation Fund for Medical Sciences (CIFMS 2016-I2M-3-004), and the Research Fund to H.Y. from Dept. of Pathology of PUMC. The authors have no affiliation to organizations that create a conflict of interest.

Author Contributions

X.-D.Y. designed and supervised the experiments; Y.A. performed the experiments; Y.A. analyzed the data; Y.H., X.L., Z.L. and J.D. gave technical support; X.-D.Y. and Y.A. wrote the manuscript; All authors read and approved the final manuscript.

Additional Information

Competing Interests: The authors declare no competing interests.

Publisher's note: Springer Nature remains neutral with regard to jurisdictional claims in published maps and institutional affiliations.



Open Access This article is licensed under a Creative Commons Attribution 4.0 International License, which permits use, sharing, adaptation, distribution and reproduction in any medium or format, as long as you give appropriate credit to the original author(s) and the source, provide a link to the Creative Commons license, and indicate if changes were made. The images or other third party material in this article are included in the article's Creative Commons license, unless indicated otherwise in a credit line to the material. If material is not included in the article's Creative Commons license and your intended use is not permitted by statutory regulation or exceeds the permitted use, you will need to obtain permission directly from the copyright holder. To view a copy of this license, visit <http://creativecommons.org/licenses/by/4.0/>.

© The Author(s) 2019